J Therm Anal Calorim (2012) 108:1067–1078
DOI 10.1007/s10973-011-2093-5

Thermal transitions and dynamics in nanocomposite hydrogels

A. Kyritsis · A. Spanoudaki · C. Pandis · L. Hartmann · R. Pelster · N. Shinyashiki · J. C. Rodríguez Hernández · J. L. Gómez Ribelles · M. Monleón Pradas · P. Pissis

ICVMTT2011 Conference Special Chapter

Abstract Hydrogels based on nanocomposites of statistical poly(hydroxyethyl acrylate-*co*-ethyl acrylate) and silica, prepared by simultaneous copolymerization and generation of silica nanoparticles by sol–gel process at various copolymer compositions and silica contents, characterized by a fine dispersion of filler, were investigated with respect to glass transition and polymer dynamics by dielectric techniques. These include thermally stimulated depolarization currents and dielectric relaxation spectroscopy, covering together broad ranges of frequency and temperature. In addition, equilibrium water sorption isotherms were recorded at room temperature (25 °C). Special attention was paid to the investigation of effects of silica on glass transition, polymer dynamics (secondary γ and β_{sw} relaxations and segmental α relaxation), and electrical conductivity in the dry systems (xerogels) and in the hydrogels at various levels of relative humidity/water content. An overall reduction of molecular mobility is observed in the nanocomposite xerogels, in particular at high silica contents. Analysis of the results and comparison with previous work on similar systems enable to discuss this reduction of molecular mobility in terms of constraints to polymeric motion imposed by interfacial polymer–filler interactions and by the formation of a continuous silica network interpenetrated with the polymer network at filler contents higher than about 15 wt%.

Keywords Poly(hydroxyethyl acrylate-*co*-ethyl acrylate)/silica hydrogels · Glass transition · Segmental dynamics · Electrical conductivity

A. Kyritsis (✉) · A. Spanoudaki · C. Pandis · P. Pissis
Department of Physics, National Technical University of Athens, Zografou Campus, 157 80 Athens, Greece
e-mail: akyrits@central.ntua.gr

L. Hartmann · R. Pelster
Department of Experimental Physics, University des Saarlandes, Saarbrücken, Germany

N. Shinyashiki
Department of Physics, Tokai University, Hiratsuka, Kanagawa 259-1292, Japan

J. C. Rodríguez Hernández · J. L. Gómez Ribelles · M. Monleón Pradas
Center for Biomaterials, Universidad Politécnica de Valencia, Valencia, Spain

Introduction

Polymer hydrogels absorb large amounts of water, owing to the presence of hydrophilic groups in their structure, and preserve at the same time their integrity, because of being cross-linked. Good biocompatibility and water permeation properties, in addition to several other good properties arising from their polymeric nature, form the basis for several applications [1, 2]. For many of these applications reduced mechanical stability at high water contents is a severe drawback. Mechanical stability can be improved by combination with a second hydrophobic polymer, often in the form of interpenetrating polymer networks (IPNs) or copolymers. For given choice of the two polymers, properties depend then sensitively on the phase morphology, which, in its turn, can be controlled by composition and preparation/processing conditions.

In previous work we employ a variety of partly complementary experimental techniques to study morphology, water sorption/diffusion, thermal transitions, dynamics and properties of biocompatible hydrogels based on poly (hydroxyethyl acrylate), PHEA, both homopolymers and

copolymers and IPNs with a hydrophobic acrylate or methacrylate [3–7]. In recent papers we focused on homogeneous statistical copolymers of PHEA and poly(-ethyl acrylate), PEA, P(HEA-*co*-EA), as candidate materials for scaffold applications [8, 9].

Next to the concept of reinforcement of the hydrogel by a hydrophobic polymer, the nanocomposite hydrogel concept is particularly attractive. In this case, the hydrogel matrix is reinforced by nanoparticles, such as clays [10–12] or silica [12], taking advantage of the well-established significant improvement of mechanical properties of polymer nanocomposites already at low filler factors. In previous work some of us reported on the preparation of PHEA/silica nanocomposite hydrogels by simultaneous polymerization and generation of silica nanoparticles by sol–gel techniques and on their structural, thermal, and mechanical characterization. The results by the various techniques indicated, in agreement to each other, strong polymer–filler interactions. The silica phase consists of elementary particles, 30–80 nm size, which form larger aggregates up to about 400 nm in size [15]. The silica nanoparticles form a continuous network interpenetrated with the organic network at filler factors higher than about 15 wt% [13, 14]. Water sorption/diffusion measurements in the same materials, both from the vapor and from the liquid phase, show, similar to other properties [13, 14], significant changes of water uptake and of water diffusion coefficient at the percolation threshold of about 15 wt% silica [15].

In the present paper we continue work along the lines described above. We focus on nanocomposites of statistical copolymers P(HEA-*co*-EA) and silica, prepared by simultaneous copolymerization and sol–gel processes, i.e., we combine in the same materials both concepts of reinforcement, by copolymerization and by nanoparticle addition. We employ two dielectric techniques, one in the temperature domain, thermally stimulated depolarization currents (TSDC), and the second in the frequency domain, the classical dielectric relaxation spectroscopy (DRS), to follow dielectric relaxations, both the segmental (primary) α relaxation associated with the glass transition and secondary relaxations, in the dry nanocomposites (xerogels), and to conclude on effects of silica on polymer dynamics and on polymer–filler interactions. In doing that we take advantage of the broad frequency and temperature ranges of DRS measurements and of the high peak resolving power of TSDC measurements. In the second part of the paper we focus on effects of water on polymer dynamics in the nanocomposites. To that aim, dielectric measurements are performed at several levels of water activity (relative humidity)/water contents at each xerogel composition, to systematically follow the evolution of dynamics and of electrical conductivity with hydration. By comparing with each other results obtained at various levels of silica content, we seek at gaining information on effects of silica on the organization of water in the hydrogels. Additional information on that point is obtained by equilibrium water sorption isotherm (ESI) measurements. Preliminary results on water sorption and molecular mobility in selected compositions, obtained by ESI and TSDC, have been reported recently [16].

Experimental

Materials

The P(HEA-*co*-EA)/silica nanocomposites were prepared by simultaneous copolymerization of 2-hydroxyethyl acrylate (HEA, 96%, Aldrich) and ethyl acrylate (EA, 99%, Aldrich), in the appropriate proportion, and generation of silica nanoparticles by sol–gel process. Benzoyl peroxide (BPO, 97%, Fluka) was used as initiator for the polymerization reaction. Tetraethoxysilane (TEOS, 98%, Aldrich) was used as silica precursor. Details of the preparation have been given elsewhere [16]. The copolymer composition was systematically varied from pure PHEA to 10/90 PHEA/PEA, whereas, for each copolymer composition, the content of silica was varied between 0 and 20 wt% in steps of 5%. The materials were prepared in the form of sheets with a thickness between 0.5 and 1.0 mm. The following code will be used throughout the paper for describing the composition of the samples and the condition of measurements: (wt% of PHEA)/(wt% of PEA)s(wt% of silica)rh(relative humidity). Results reported in this paper refer to the copolymer compositions 100/0, 90/10, 70/30, and 10/90.

Methods

For ESI measurements, samples were allowed to equilibrate to constant mass over saturated salt solutions in sealed jars at controlled relative humidity rh (water activity α_w) at room temperature (25 °C). rh was adjusted by using saturated aqueous salt solutions [5, 7]. The water content h, defined as the ratio of the mass of water in the hydrogel to the mass of the dry sample (dry basis), was determined by weighing [5]. A Bosch SAE 200 balance with 10^{-4} g sensitivity was employed for these measurements. Dry masses were determined by drying to constant weight in vacuum (5×10^{-2} Torr) for at least 24 h at 80 °C.

TSDC is a special dielectric technique in the temperature domain, which consists of measuring the thermally activated release of stored dielectric polarization. The method corresponds to measuring dielectric loss as a function of temperature at a fixed low frequency in the range 10^{-2}–10^{-4} Hz (equivalent frequency of TSDC

measurements [4]). The technique provides means for a quick characterization of the overall dielectric behavior of the material under investigation and is characterized by high sensitivity and high peak resolving power. A Novocontrol sample cell in combination with a Novocontrol Quatro Cryosystem and a 617 programmable Keithley electrometer were used for TSDC measurements in the temperature range from −150 to 30 °C. Measurements were performed on samples at various levels of water content h. To that aim, the sample was equilibrated to constant mass in a closed jar with varying relative humidity rh prior to dielectric measurement and the mass of the sample was measured before and after the measurement. The relative humidity of equilibrating the sample or the mean value of water content (average value before and after the measurement) will be used throughout the paper for characterizing the hydration state of the sample at each dielectric measurement. Details of the TSDC method and of the measuring procedure have been given elsewhere [4, 6, 16].

For DRS measurements [17] the complex dielectric function (also known as dielectric permittivity or dielectric constant), $\varepsilon^*(\omega) = \varepsilon'(\omega) - i\varepsilon''(\omega)$, was determined as a function of frequency (10^{-1}–10^6 Hz) at constant temperature (−150 to 80 °C in small steps, depending on the process under investigation), controlled to better than ±0.1 °C, using a Novocontrol Alpha Analyzer in combination with a Novocontrol Quatro Cryosystem. Similar to TSDC, measurements were performed on samples at various levels of rh/h. Samples for TSDC and DRS measurements were circular sheets with 15 mm diameter and thickness between 0.5 and 1.0 mm.

Results

Xerogels

DRS and TSDC measurements in P(HEA-*co*-EA) in previous work [9] showed that the dielectric response is dominated by PHEA. The results in the dry copolymers (xerogels) show the presence of a secondary γ relaxation at low temperatures, arising from the motion of the polar group –CH_2–CH_2–OH in the side chain of the HEA monomer [5], and the primary (segmental) α relaxation associated with the glass transition at higher temperatures. With the first traces of water the β_{sw} relaxation appears, assigned to the association of one water molecule with the polar groups of two adjacent side chains [4–7]. The results obtained with the dry copolymers showed that these are homogeneous at nanometer level, the characteristic length of the glass transition [18], except for PEA-rich compositions, which are microphase-separated. In this section we follow dielectric relaxations in the nanocomposite xerogels with silica content as a variable to conclude on effects of silica on polymer dynamics and on polymer–filler interactions.

Figure 1 shows DRS results at the example of the 70/30 copolymer, real and imaginary part of the dielectric function against frequency, $\varepsilon'(f)$ and $\varepsilon''(f)$, respectively, to follow effects of silica on the segmental α relaxation (dynamic glass transition [18]). These and similar results were analyzed by fitting the Havriliak–Negami (HN) model function [19]

$$\varepsilon^*(\omega) - \varepsilon_\infty = \frac{\Delta\varepsilon}{[1 + (i\omega\tau)^{1-\alpha}]^\beta} \quad (1)$$

to the experimental data. In this expression $\Delta\varepsilon$ is the dielectric strength, $\Delta\varepsilon = \varepsilon_s - \varepsilon_\infty$, where ε_s and ε_∞ are the low- and high-frequency limits of ε', respectively, τ is the relaxation time, $\tau = 1/2\pi f_{HN}$, where f_{HN} is a characteristic frequency closely related to the loss peak frequency f_{max}, and α, β are shape parameters describing the shape of the $\varepsilon''(\omega)$ curve, $0 < \alpha \leq 1$ and $0 < \beta \leq 1$. Depending on the shape of the data at each temperature and relative humidity of measurements, a more complex expression was used, such as a sum of one HN term for α and a term for conductivity in Fig. 1. Analysis provides information on the time scale, the strength and the shape of each relaxation process [4, 19]. We make repeatedly use of this type of analysis in the following. Where possible, however, we extract information directly from the raw data for a more unbiased discussion.

We observe in Fig. 1 that the loss peak in $\varepsilon''(f)$ and the corresponding step in $\varepsilon'(f)$ shift slightly to lower frequencies and become broader with increasing silica content, i.e., segmental dynamics becomes slower and more distributed in the nanocomposites, which was confirmed and quantified by analysis. Similar results were obtained also with the other copolymer compositions. The slowing down of the α relaxation in the nanocomposites was confirmed also by TSDC [16]. These results agree well with those of differential scanning calorimetry (DSC) measurements in PHEA–silica nanocomposites [13]. Moreover, they show that the slight slowing down of the α relaxation and the corresponding increase of the glass transition temperature T_g in the nanocomposites, observed so far for the PHEA–silica nanocomposites [13], is true also for the copolymer nanocomposites. The DSC results showed also a decrease of the heat capacity step at the glass transition ΔC_p (normalized to the same polymer fraction) in the PHEA–silica nanocomposites, as compared to neat PHEA, which was interpreted in terms of a fraction of polymer being immobilized, i.e., making no contribution to the glass transition. The counterpart of ΔC_p in dielectric measurements is the dielectric strength $\Delta\varepsilon$ of a relaxation, obtained

by analysis, as described above. A representative value of $\Delta\varepsilon$ is given by the difference of ε' at lower and higher frequencies with respect to the frequency region of the relaxation [20]. The data in Fig. 1 for the 70/30 copolymer and similar data for the other copolymer compositions, not shown here, suggest that $\Delta\varepsilon$ decreases in the nanocomposites. This is an interesting observation in the frame of an ongoing discussion on the effects of the filler on structure and dynamics of the polymer matrix in polymer nanocomposites, as revealed by various techniques. We will come back to this point later in the "Discussion" section.

Figure 2 shows results similar to Fig. 1, now at the example of the 90/10 copolymer and at a lower temperature, −80 °C, to follow effects of silica on the secondary γ relaxation. We observe that the relaxation becomes slightly faster with increasing silica content, whereas its magnitude (dielectric strength $\Delta\varepsilon$) decreases. To further quantify and generalize this observation we show in Fig. 3 results for $\Delta\varepsilon$ of the γ relaxation, obtained by analysis, against silica content for three matrix compositions. $\Delta\varepsilon$ decreases with increasing silica fraction by far more than it would be expected by normalization to the same polymer matrix, in

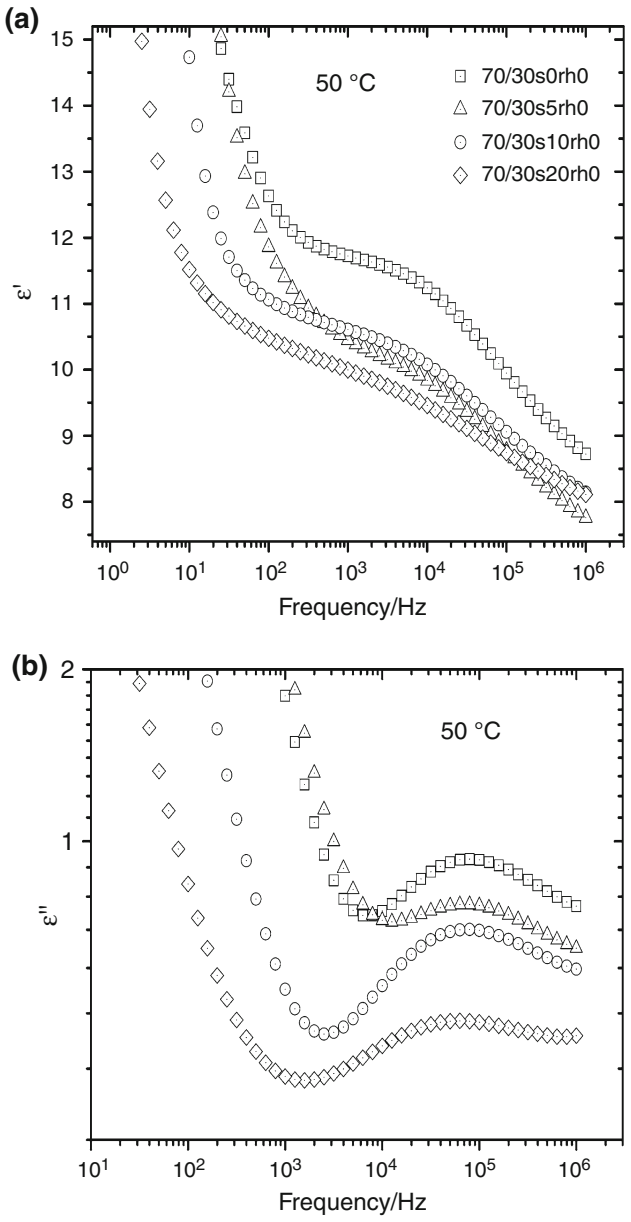

Fig. 1 Real (**a**) and imaginary (**b**) part of the dielectric function against frequency, $\varepsilon'(f)$ and $\varepsilon''(f)$, respectively, for the samples indicated on the plot at 50 °C

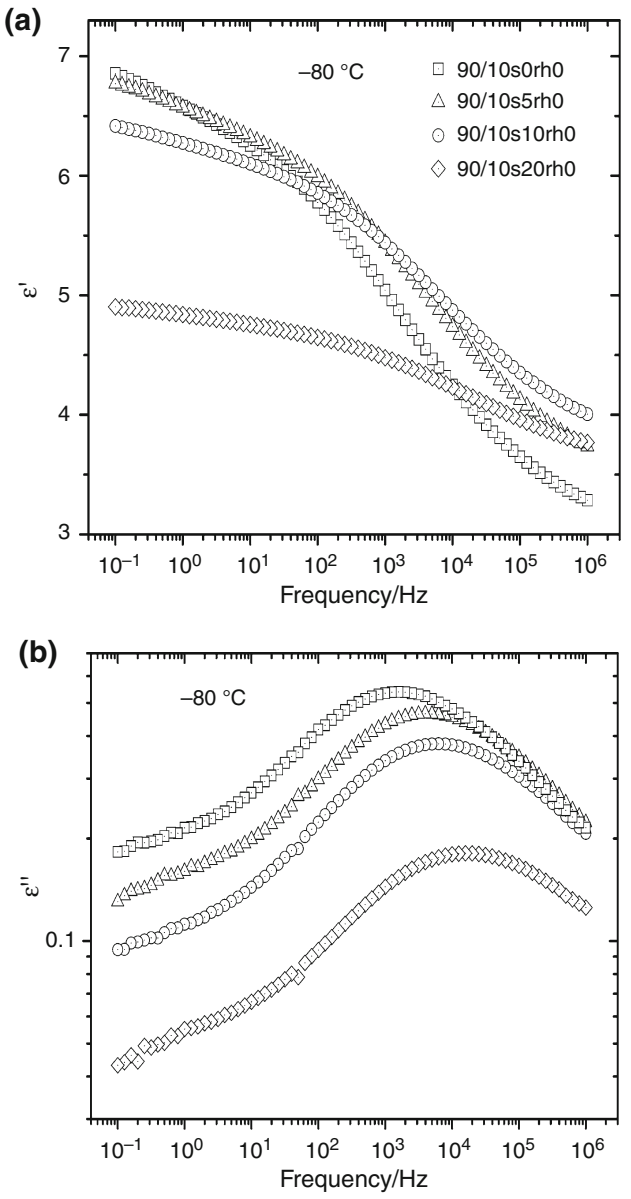

Fig. 2 Real (**a**) and imaginary (**b**) part of the dielectric function against frequency, $\varepsilon'(f)$ and $\varepsilon''(f)$, respectively, for the samples indicated on the plot at −80 °C

particular at the highest silica fraction of 20 wt%. To further follow this point we compare in the inset to Fig. 3 experimental and calculated results for $\Delta\varepsilon$ of the γ relaxation for neat PHEA at −100 °C. The experimental results were obtained by the HN analysis described above (Eq. 1). The calculated results were obtained by using the Maxwell-Garnett effective medium model [21]. By assuming that the dielectric function of the silica particles has a real and constant value ε_p (=2.2), whereas the polymer matrix shows a relaxation with dielectric strength $\Delta\varepsilon_m$ and a high frequency value of the dielectric function ε_∞ (=3.3 and 2.9, respectively, obtained by HN analysis), the dielectric strength $\Delta\varepsilon_{eff}$ of the relaxation can be calculated within this model to

$$\Delta\varepsilon_{eff} = \Delta\varepsilon_m \cdot \left[1 - 3 \cdot f \frac{\Delta\varepsilon_m + \varepsilon_\infty - \varepsilon_p + \frac{3\cdot\varepsilon_p\cdot\varepsilon_\infty}{\alpha}}{\alpha + (2+f)\cdot\Delta\varepsilon_m}\right] \quad (2)$$

In this equation, f is the volume fraction of the particles

$$f = \frac{1}{1 + \frac{\rho_p}{\rho_m}\frac{(1-x)}{x}} \quad (3)$$

where ρ_p (=2.2 g/cm^3 [14]) is the density of the silica particles, ρ_m the density of the matrix (=1.3 g/cm^3 [14]), x the mass fraction of silica and $\alpha = (2+f)\cdot\varepsilon_\infty + (1-f)\cdot\varepsilon_p$. Results similar to those shown in the inset to Fig. 3 have been obtained also with the other copolymer compositions: experimental $\Delta\varepsilon$ values of the γ relaxation are smaller than calculated $\Delta\varepsilon_{eff}$ values at high silica content. Several reasons can be at the origin of this observation: (1) The Maxwell-Garnett model, similar to other effective medium models, is valid only at low filling factors; the model assumes a dispersion of isolated silica particles and, thus, it fails to describe data at high filling factors, where silica particles have been shown to agglomerate forming a continuous, percolating network, as described in "Introduction" section [13–15]. (2) The reduction of $\Delta\varepsilon$ is related to the immobilization of a fraction of polymer close to the nanoparticles, as suggested by DSC measurements in PHEA–silica nanocomposites [13] and also by the DRS data for the α relaxation in Fig. 1 (although it is difficult to imagine that immobilization affects also local relaxations). (3) Finally, $\Delta\varepsilon$ of the γ relaxation is reduced in the nanocomposites due to a specific hydrogen or covalent bonding interaction of the polar group responsible for this relaxation, –CH_2–CH_2–OH in the side chain of the HEA monomer, with hydroxyls on the silica surface (although the effect should be then less pronounced at high silica fractions where agglomeration occurs). We will continue this discussion later on the basis of additional results to be reported below.

As indicated by the results above, effects of silica on the time scale of the α and γ relaxations are weak (in contrast to effects on the dielectric strength, Fig. 3). This observation is summarized at the example of neat PHEA in the Arrhenius plot of Fig. 4. The (nominally) dry samples were allowed to absorb traces of water during installation in the measuring equipment (compare "Experimental" section), so that, next to α and γ, a weak β_{sw} relaxation was recorded and analyzed. TSDC data, included to the plot at the equivalent frequency of 1.6 mHz, corresponding to a relaxation time of 100 s [3], for the α and the β_{sw}

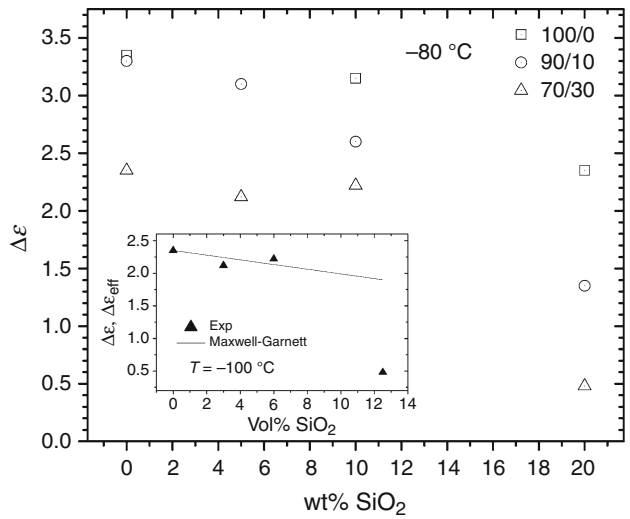

Fig. 3 Dielectric strength $\Delta\varepsilon$ of the γ relaxation obtained by fitting analysis against silica fraction for three matrix compositions indicated on the plot. The *inset* compares experimental and calculated results for $\Delta\varepsilon$ of the γ relaxation using the Maxwell-Garnett model (Eq. 1) at the example of neat PHEA at −100 °C

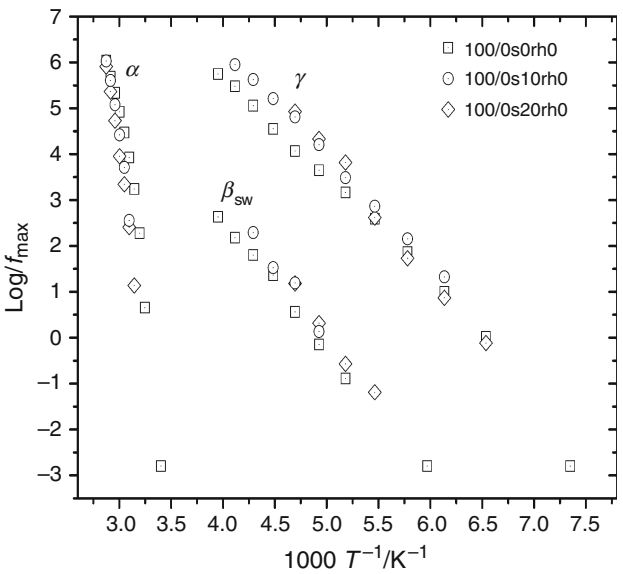

Fig. 4 Arrhenius plot of the dielectric relaxations for the compositions indicated on the plot. Included are also TSDC data at the equivalent frequency of 1.6 mHz

relaxations (the γ relaxation being out of the temperature range of our TSDC equipment) are in good agreement to the DRS data, enabling to practically extend the range of measurements to lower frequencies. We observe in Fig. 4 that α becomes slightly slower and γ slightly faster in the nanocomposites. We will comment on the behavior of the β_{sw} relaxation in the next section. We will not discuss here the temperature dependence of the time scale of the relaxations (obviously Arrhenius for the local γ and β_{sw} relaxations and Vogel–Tammann–Fulcher (VTF) for the cooperative α relaxation [18]).

As suggested by the results in Fig. 1b, electrical conductivity of the xerogels decreases with increasing silica content. To further follow and quantify this point, ac conductivity σ_{ac} (actually real part of the complex conductivity) was calculated from the measured dielectric loss $\varepsilon''(\omega)$ by [17, 22]

$$\sigma_{ac}(\omega) = \varepsilon_o \omega \varepsilon''(\omega) \quad (4)$$

where ε_o is the permittivity of free space. At temperatures higher than T_g, the $\sigma_{ac}(\omega)$, or $\sigma_{ac}(f)$, plots (not shown here) exhibit at low frequencies plateau (frequency independent) values, which give dc conductivity σ, followed by an increase with increasing frequency [22]. In the following we focus on the dependence of σ on silica content and temperature. Figure 5 shows T_g-scaled Arrhenius plots of conductivity in neat PHEA xerogels at different silica contents. Conductivity decreases in the nanocomposites, in particular at high silica contents. Although no fittings are shown in Fig. 5, it is clear that, at each composition, the points follow a concave VTF behavior, indicating that the proton conductivity mechanism giving rise to the results shown in Fig. 5 is governed by the motion of the polymeric chains [22]. It is interesting that conductivity becomes more Arrhenius-like at the highest silica fraction of 20 wt%. Similar results were obtained also with the various copolymer compositions. For the construction of these plots, T_g values determined by TSDC were employed.

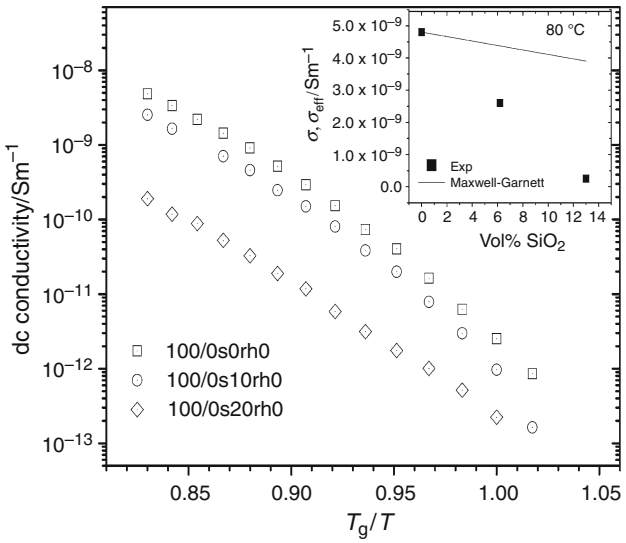

Fig. 5 T_g-scaled Arrhenius plot of dc conductivity, σ, in the nanocomposite xerogels indicated on the plot. The *inset* compares experimental and calculated results for σ using the Maxwell-Garnett model (Eq. 5) at 80 °C

The T_g-scaled presentation was used in Fig. 5, as it enables to distinguish between effects on conductivity arising from charge carrier concentration and effects arising from chain mobility. There should be, however, also an effect, even if small, arising from the reduction of the (conducting) polymer fraction with increasing silica content. To properly consider this point, the inset to Fig. 5 shows experimental and calculated results for σ in PHEA xerogels against silica content at 80 °C, well above T_g. The calculated results were obtained by using again the Maxwell-Garnett effective medium model [21]. By assuming isolated, non-conducting nanoparticles ($\sigma_p = 0$), the effective conductivity σ_{eff} can be calculated within this model to

$$\sigma_{eff} = \sigma_m \left(1 - 3\frac{f}{2+f}\right) = 2 \cdot \sigma_m \frac{1-f}{2+f} \quad (5)$$

For the conductivity of the matrix, σ_m, we used the experimentally determined value of 4.85×10^{-9} S/m. Similar results were obtained also for the various copolymer compositions. The reduction of conductivity in the nanocomposites is much larger than predicted by the Maxwell-Garnett (and other similar effective medium models, not discussed here). Agglomeration and formation of a continuous silica network, cutting more paths for charge carrier motion than finely dispersed nanoparticles, is a possible explanation for this behavior. Reduction of molecular mobility of the polymer matrix/immobilization of a polymer fraction, as suggested by results reported above, is another reasonable explanation. We will take up this point again in the "Discussion" section.

Hydrogels

Results for ESI measurements at three copolymer compositions and two silica contents for each of them are shown in Fig. 6. They extend results obtained in previous work with P(HEA-*co*-EA) copolymers [9], PHEA/silica nanocomposites [15], and selected compositions of the present work [16]. In Ref. [15] results in PHEA/silica nanocomposites were extensively analyzed in terms of sorption by PHEA and by silica. The data in Fig. 6 were fitted by the Guggenheim–Anderson–DeBoer (GAB) equation [5, 7]

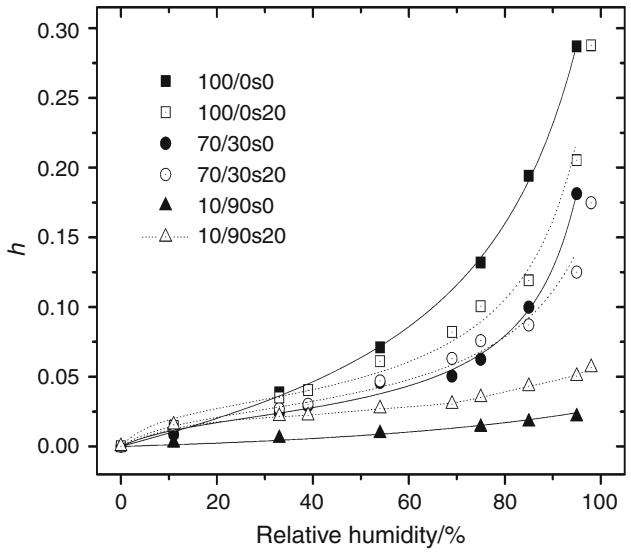

Fig. 6 Water content h against relative humidity rh for the samples indicated on the plot at 25 °C. The *lines* are fittings of Eq. 6 to the experimental data

$$\frac{h(\alpha_w)}{h_m} = \frac{cf\alpha_w}{(1-f\alpha_w)[1+(c-1)f\alpha_w]} \quad (6)$$

In this equation α_w is the water activity (relative humidity rh), h_m is the first monolayer sorption capacity, c is the activity of the water molecules in the first monolayer referred to the activity of the molecules in the second and successive adsorbed layers, and f is the activity of the molecules in the second and successive adsorbed layers referred to the activity of condensed liquid water, at the same temperature and pressure. At each copolymer composition and low values of rh, water uptake is larger in the corresponding nanocomposite, reflecting the high sorption capacity of silica at low rh values (sorption isotherm of type I in the Brunauer classification [15]). The combination of water clustering in the polymer matrix at high rh values, leading to an upward swing of the isotherm, with constraints imposed to swelling by the formation of a continuous silica network [13–15], may result in a reversal of this behavior at higher rh values, depending on the hydrophilicity of the copolymer matrix. This reversal occurs at about 35% rh in neat PHEA and at about 80% rh in 70/30, whereas it is absent in the more hydrophobic 10/90 composition. These results are also of practical significance in designing materials with predicted water uptake behavior. In is interesting to note with respect to effects of silica on water clustering that detailed analysis of the sorption data in PHEA/silica nanocomposites revealed that, for the same relative humidity, the mean size of water clusters decreases at high silica contents [15].

Effects of water on glass transition and polymer dynamics in the nanocomposite hydrogels were followed by DRS and TSDC measurements at various levels of relative humidity (corresponding to various levels of water content). We recall that the TSDC peak temperature of the α relaxation, T_α, is a good measure of the calorimetric glass transition temperature T_g [3, 5, 6]. An example of measurements is shown in Fig. 7, where we can follow effects of water on the secondary γ and β_{sw} relaxations (a) and on the segmental α relaxation (b) in the 70/30s20 composition. We observe in Fig. 7a how the β_{sw} process, at lower frequencies than γ, emerges with the first traces of water and becomes significant in magnitude already at low water contents (comparable to γ already at rh=11%) and also faster. The γ process is less sensitive to water content. At high hydrations the two processes merge and we observe

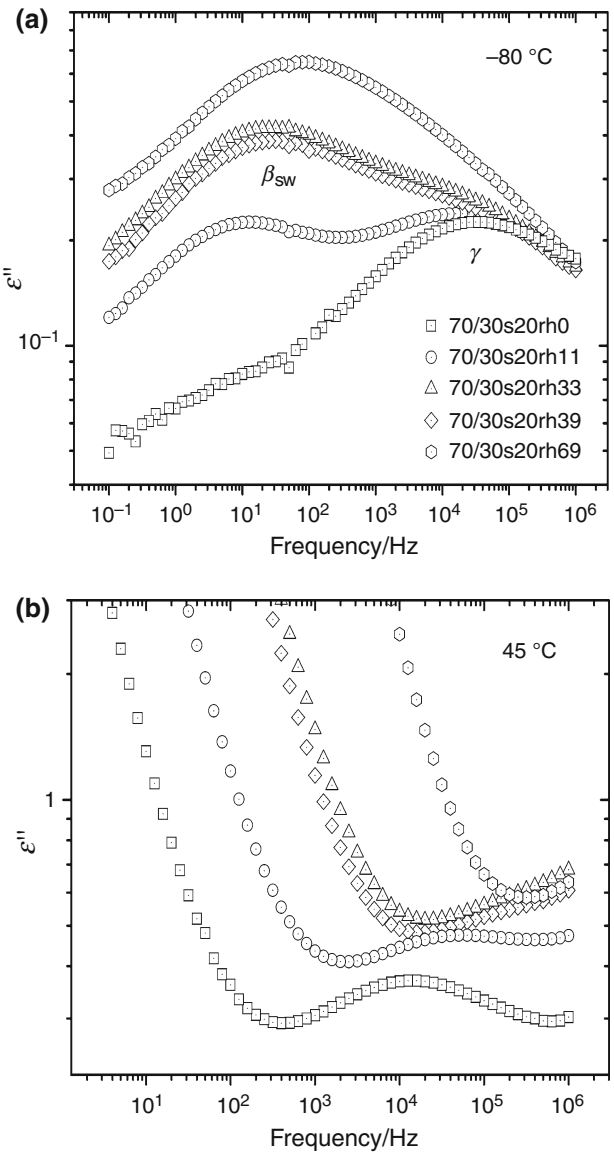

Fig. 7 Dielectric loss against frequency, $\varepsilon''(f)$, for 70/30s20 at −80 °C (**a**) and at 45 °C (**b**), at several values of relative humidity indicated on the plot

only the β_{sw} process, because of its higher strength. The shift of the α relaxation to higher frequencies with increasing rh in Fig. 7b is much faster than for the secondary relaxations in Fig. 7a. However, conductivity, which gives rise to the steep wing at low frequencies, increases significantly with increasing level of hydration and, as a result, the α relaxation can be resolved only at low levels of rh. This limitation does not hold in the case of TSDC measurements, probably because of the separation of the stimulus (polarization) and the response (depolarization) steps in this kind of measurements. As a result, the α process can be followed also at high levels of rh and h [3, 5, 6]. Please note that this is true for the time scale (temperature position) of the relaxation, whereas its magnitude (dielectric strength) increases significantly due to conductivity contributions, as clearly shown for PHEA hydrogels in a previous work [3].

Results similar to those shown in Fig. 7 were recorded on samples with different copolymer composition and silica content. Results can be compared to each other with respect to the effects of silica content in the form of raw data, such as in Fig. 7, or after Havriliak–Negami analysis (Eq. 1). Comparison becomes unambiguous with respect to the magnitude of the γ and α relaxations already at relatively low rh values, for different reasons: the γ relaxation disappears then practically in the growing β_{sw} relaxation (Fig. 7), whereas conductivity contributes significantly to the TSDC α response (without, however, any significant effect on the time scale of the response, as mentioned above). Comparison shows that the time scale of the three relaxations, γ, β_{sw}, and α, is not significantly affected by silica content, in the sense that, for the same level of rh, the relaxations are plasticized by water to approximately the same degree independently of silica content. Small differences are due to the fact that for a given copolymer composition at a given rh, water content h depends on silica content, in particular at high levels of rh, as demonstrated in Fig. 6. Please note, however, that the first water (at primary hydration sites) is a more effective plasticizer than clustered water [5].

In contrast to the time scale of dipolar relaxations, dc conductivity σ depends sensitively on silica content at each level of rh/h. This is demonstrated in Fig. 8 at the example of the 70/30 copolymer. For both silica contents, 0 and the highest one of 20%, σ increases significantly with rh, whereas at each rh, σ is by about two orders of magnitude smaller in the nanocomposite hydrogel. This large deviation cannot be due to the small differences in the corresponding water sorption isotherms (Fig. 6), as it is observed also in the xerogels. Moreover, in the rh values of Fig. 8, h is slightly larger in 70/30s20, the composition with lower σ, as compared to 70/30s0. As observed also for the PHEA xerogels in Fig. 5, σ becomes more Arrhenius-like at high

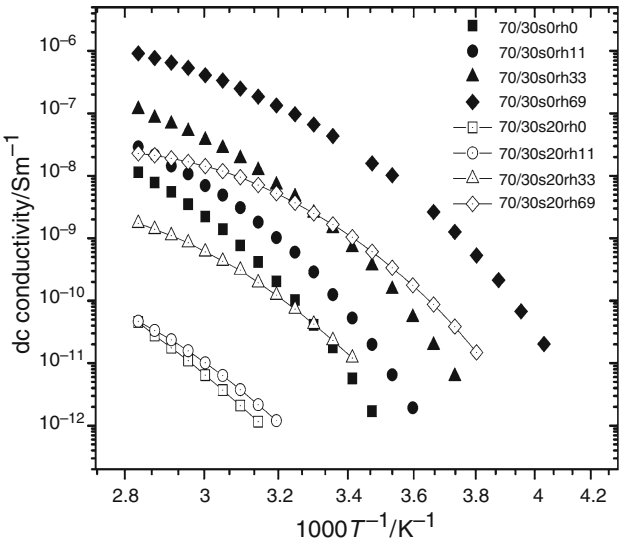

Fig. 8 Arrhenius plot of dc conductivity, σ, in the nanocomposite hydrogels and the rh indicated on the plot

silica contents. It is interesting that this behavior changes back to VTF-like (concave temperature dependence) with increasing rh. This point should be further followed and quantified in future work, by analyzing the data in Fig. 8 and similar data in other copolymer compositions in terms of fragility [23]. The different behavior of conductivity, on the one hand, and of dipolar relaxations, on the other hand, with respect to effects of silica, can be explained by considering the different spatial scale of the two types of processes (macroscopic against local), as will be discussed in the next section. Characteristic values of σ, measured on 70/30s0 and 70/30s20 samples, together with the corresponding values of h and ε' (at $f = 1$ MHz) obtained at various rh are given in Table 1.

Discussion

Figure 9 summarizes some of the results on the effects of silica on polymer dynamics in the xerogels presented above and helps to further clarify some points. It shows isochronal (constant frequency) plots of the temperature dependence of ε' at the example of the 70/30 xerogel at three silica contents. A high frequency has been selected for the presentation to get rid of conductivity effects. Temperature trends are significant in Fig. 9 and representative also for other copolymers, whereas absolute values depend on copolymer composition. The increase of $\varepsilon'(T)$ at low (subzero) temperatures originates from the γ relaxation, as confirmed also by the corresponding $\varepsilon''(T)$ plot, not shown here, and is clearly smaller for the xerogel with 20% silica, in agreement with results reported above (Figs. 2, 3). The most striking result in Fig. 9 is the significantly

Table 1 Characteristic values of water content, h, dc conductivity, σ, and dielectric permittivity, ε' (measured at 10^6 Hz) obtained on samples 7030S0 and 7030S20 at 25 °C (room temperature) with varying relative humidity, rh

rh	7030S0			7030S20		
	h	σ/Sm^{-1}	ε' ($f = 1$ MHz)	h	σ/Sm^{-1}	ε' ($f = 1$ MHz)
0	0.000	4.1×10^{-11}	7.40	0.000	2.1×10^{-13}	6.55
11	0.007	2.8×10^{-10}	8.35	0.012	4.5×10^{-13}	7.30
33	0.022	2.4×10^{-9}	9.05	0.027	5.2×10^{-11}	9.15
69	0.054	6.5×10^{-8}	14.92	0.063	3.5×10^{-9}	10.63

smaller increase of $\varepsilon'(T)$ in this xerogel at higher temperatures, corresponding to the segmental α relaxation (dynamic glass transition), even after normalization to the same polymer fraction. This means that molecular motions in the nanocomposite xerogels remain frozen at temperatures higher than T_g and become gradually unfrozen at higher temperatures [20, 24]. The results may suggest a levelling off of $\varepsilon'(T)$ at the highest temperature of measurements in Fig. 9 in 70/30s0 and 70/30s10 against a steady increase in 70/30s20, supporting the concept of constraints imposed to the motion of polymeric chains by the silica nanoparticles and release of these constraints at higher temperatures, similar to results obtained previously with rubbery epoxy networks/POSS nanocomposites [25]. This point should be further followed by extending measurements to higher temperatures in future work.

Most of the results obtained with the P(HEA-*co*-EA)/silica nanocomposite hydrogels in the present paper (as well as with some of these materials in [16] and with

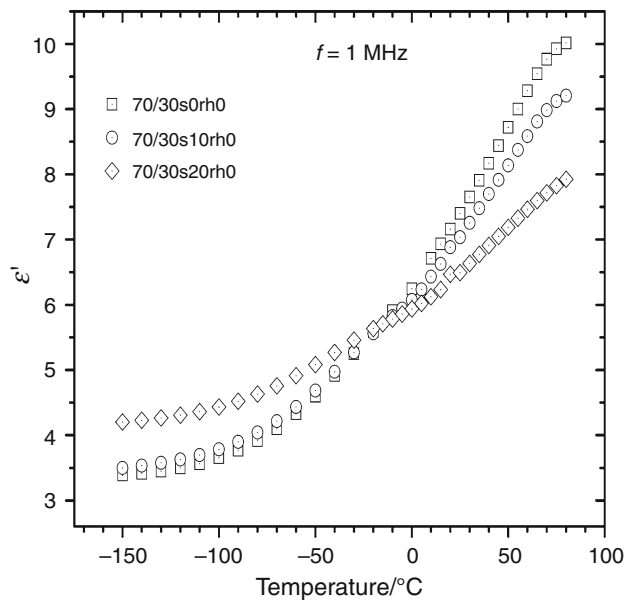

Fig. 9 Isochronal plots of the real part of the dielectric function against temperature, $\varepsilon'(T)$, for the samples indicated on the plot at 1 MHz

PHEA/silica nanocomposite xerogels [13, 14] and hydrogels [15]) can be explained using (1) the concept of constraints imposed to the motion of polymeric chains by the presence of and interactions with the silica nanoparticles; (2) the concept of silica nanoparticle aggregation and formation of a continuous network at high filler content [13–15]. It has been shown in previous work by systematically comparing systems with different quality of filler dispersion and different strength of polymer–filler interactions that the reduction of molecular mobility of the polymer matrix becomes more pronounced with increasing quality of filler dispersion and increasing strength of polymer–filler interactions [24, 26, 27]. Polymer–filler interactions are expected to arise here from hydrogen bonding between the carbonyls and the hydroxyls in the polymer side chains and silanols on the silica surface. FTIR measurements failed to reveal heterogeneous condensation reactions between the HEA monomers and the silanols in PHEA/silica nanocomposites, since the characteristic peaks for the expected Si–O–C bond in that case overlap the absorption interval of the Si–O–Si bond [14]. In addition to the rather general concept of reduction of molecular mobility due to constraints imposed to the motion of the polymeric chains by interfacial polymer–filler interactions described above, the formation of a continuous silica network interpenetrated with the polymer network at silica contents higher than about 15 wt% is a specific feature of the PHEA–silica nanocomposites [13–15]. An interesting question is which of the results need for explanation (and, thus, provide confirmation for) the first or the second or both concepts.

The slight slowing down and broadening of the segmental α relaxation observed by DRS and the corresponding increase of T_g observed by TSDC, also in [16], can be explained by constraints to the motion of the polymeric chains arising from interfacial interactions. Results are similar to those observed in PHEA/silica nanocomposites by DSC [13]. The reduction of the strength of the α relaxation in the nanocomposites, corresponding to the reduction of ΔC_p at the glass transition, observed in PHEA/silica nanocomposites by DSC [13], would suggest that a fraction of polymer is immobilized in the interfacial layer, making no contribution to the α relaxation and the

glass transition. Similar results, with respect to the DSC–DRS comparison, have been obtained in polyurethane/clay nanocomposites [20]. Contrary to that, DSC results in poly(dimethylsiloxane)/silica [24] and natural rubber/silica nanocomposites [26] show a systematic reduction of ΔC_p at the glass transition without any reduction of the magnitude of the corresponding DRS response (which consists then of two α relaxations, one characteristic of the bulk polymer and a slower one arising from the interfacial polymer), and this apparent contradiction has been explained in terms of the Adam–Gibbs model for the glass transition [26]. This point should be further followed in future work, also in relation to results reported recently on the impact of annealing on the dynamic glass transition in thin polymer layers [28]. The DSC results for the silica content dependence of ΔC_p in PHEA/silica nanocomposites showed a change of the behavior at the percolation threshold for the formation of a continuous silica network [13]. This point could not be followed by dielectric techniques in the copolymer-based nanocomposites investigated here.

In contrast to α relaxation, effects of silica on the time scale and the strength of the local γ relaxation (Figs. 2, 3) cannot be described in terms of the general concept of reduction of polymer mobility in the nanocomposites described above, but are rather due to specific covalent or hydrogen bonding interaction of the polar group responsible for the relaxation, $–CH_2–CH_2–OH$ in the side chain of the HEA monomer, with silanol groups (compare the comment on the relevant FTIR results [14] above). This is consistent with the reduction of the strength, shown in Fig. 3, and the concomitant slight acceleration of the relaxation. Support for this explanation comes from water sorption measurements in PHEA/silica nanocomposites, which show that less water is sorbed in the nanocomposites than it would follow from additivity already at low rh values, suggesting that a fraction of sorption sites is lost (Fig. 3 in [15]).

Effects of silica on electrical conductivity (Figs. 5, 9) are strong, in particular at high silica contents above the percolation threshold for the formation of a continuous silica network (Fig. 5). This would favor formation of the silica network as their origin rather than immobilization of the polymer in an interfacial layer around the nanoparticles alone. It is also rather difficult to imagine, in terms of Maxwell-Garnett (inset to Fig. 5) or any other effective medium theory, how a drop of conductivity by two orders of magnitude would result solely from such immobilization. On the other hand, conductivity changes in the xerogels from VTF-like to Arrhenius-like at high silica content (Fig. 5) and then, in the hydrogel based on that nanocomposite, back to VTF-like with increasing water content (Fig. 8). This behavior reflects the stiffening of the polymer matrix imposed by the interpenetrated silica network in the xerogels and then the relaxation of the structure in the hydrogels. The VTF behavior suggests that conductivity is governed by the motion of the polymeric chains [22]. In addition, the significant drop of conductivity at 20% silica content in the T_g-scaled presentation of Fig. 5 suggests that this drop is related to reduction of segmental mobility rather than of charge carrier concentration [22].

So far it seems that there is a contradiction between the significant effect of silica on conductivity (Figs. 5, 8), as compared to the only slight one on the time scale of the α relaxation (Fig. 4), on the one hand, and the experimental evidence that conductivity is governed by the motion of the polymeric chains, on the other hand. These two apparently inconsistent pictures can be reconciled, if we consider that the α relaxation in Fig. 4 refers solely to the mobile polymer phase, whereas conductivity is affected by mobility of the whole polymer matrix. So, there is also an effect of immobilization of a polymer fraction on conductivity, in addition to the main one of formation of a continuous silica network, in the sense that diffusion of charge carriers through the immobilized polymer fraction is much slower that through the mobile one. The reduction of conductivity at high silica content resembles the reduction of water diffusion coefficient in PHEA/silica nanocomposites at high silica contents (Fig. 12 in [15]), in terms of silica content dependence, although to a smaller degree there. Both processes, electrical conductivity and water diffusion, are characterized by macroscopic spatial scales, in contrast to the dipolar γ, β_{sw}, and α relaxations, and, in a sense, the moving ions, respectively, water molecules probe the local morphology. Finally, we should mention in this connection that also other observations in the PHEA/silica nanocomposites can be better explained by the formation of a continuous silica network rather than immobilization in an interfacial polymer layer around the nanoparticles, namely suppression of swelling in [15] and significant increase of elasticity modulus in [14].

Conclusions

Two dielectric techniques, TSDC and DRS, covering together broad ranges of frequency and temperature, were employed to study glass transition and polymer dynamics in hydrogels based on nanocomposites of statistical poly(HEA-*co*-EA) and silica. The nanocomposites were prepared by simultaneous copolymerization and generation of silica nanoparticles by sol–gel process at various copolymer compositions and silica contents and they were characterized by a fine dispersion of filler. In the dry nanocomposites (xerogels), the segmental (primary) α relaxation associated with the glass transition, secondary relaxations and electrical conductivity were followed and

the results were analyzed and discussed in terms of effects of silica on polymer dynamics and on polymer–filler interactions. In the hydrogels, dielectric measurements were performed at several levels of water activity (relative humidity)/water contents at each copolymer composition and silica content, to systematically follow the evolution of dynamics and of electrical conductivity with hydration. In addition, equilibrium water sorption isotherms were recorded at room temperature (25 °C).

The following conclusions can be drawn from the results for the xerogels.

1. The segmental dynamics becomes slightly slower and more distributed with increasing silica content. At the same time the dielectric strength $\Delta\varepsilon$ of the relaxation decreases. These results can be understood in terms of a fraction of polymer being immobilized around the silica nanoparticles, due to polymer–filler interactions, in agreement with DSC results.
2. The secondary γ relaxation becomes slightly faster with increasing silica content, whereas its magnitude (dielectric strength $\Delta\varepsilon$) decreases. Acceleration is explained in terms of increase of free volume due to looser molecular packing of the chains, whereas the reduction of $\Delta\varepsilon$ arises from a specific hydrogen or covalent bonding interaction of the polar group responsible for this relaxation, $–CH_2–CH_2–OH$ in the side chain of the HEA monomer, with hydroxyls on the silica surface. Support for the latter is provided by water uptake measurements in PHEA/silica nanocomposites, which suggest that a fraction of sorption sites is lost [15].
3. Conductivity is governed by the motion of the polymeric chains. It decreases with increasing silica content and, at the same time, becomes more Arrhenius-like. Effects of silica on conductivity are strong, in particular above the percolation threshold for the formation of a continuous silica network. This would favor formation of the silica network as their origin rather than immobilization of the polymer in an interfacial layer around the nanoparticles alone.

The main results for the hydrogels can be summarized as follows.

1. At each copolymer composition and low values of rh, water uptake is larger in the nanocomposites, as compared to the neat matrix, reflecting the high sorption capacity of silica at low rh values. A reversal of this behavior may be observed at higher rh values, depending on the hydrophilicity of the copolymer matrix, due to constraints to swelling imposed by the silica nanoparticles. These results are also of practical significance in designing materials with predicted water uptake behavior.
2. At each composition, both segmental and local dynamics become faster with increasing rh and conductivity increases. It is interesting that conductivity becomes again VTF-like, a point which should be further followed and quantified in future work by analyzing data in terms of fragility.

Acknowledgements The research leading to these results has received support from the program for basic research PEBE 2010 funded by the National Technical University of Athens.

References

1. Peppas NA, editor. Hydrogels in medicine and pharmacy, vol. I. Boca Raton, FL: CRC Press; 1986.
2. Stoy V, Kliment C. Hydrogels: speciality plastics for biomedical and pharmaceutical applications. Basel: Technomic; 1996.
3. Kyritsis A, Pissis P, Gomez Ribelles JL, Monleon Pradas M. Depolarization thermocurrent studies in poly(hydroxyethyl acrylate)/water hydrogels. J Polym Sci Part B Polym Phys. 1994; 32:1001–8.
4. Kyritsis A, Pissis P, Grammatikakis J. Dielectric relaxation spectroscopy in poly(hydroxyethyl acrylate)/water hydrogels. J Polym Sci Part B Polym Phys. 1995;33:1737–50.
5. Kyritsis A, Pissis P, Gomez Ribelles JL, Monleon Pradas M. Polymer-water interactions in poly(hydroxyethyl acrylate) hydrogels studied by dielectric, calorimetric and sorption isotherm measurements. Polym Gels Netw. 1995;3:445–69.
6. Gallego Ferrer G, Monleon Pradas M, Gomez Ribelles JL, Pissis P. Swelling and thermally stimulated depolarization currents in hydrogels formed by interpenetrating polymer networks. J Non-Cryst Solids. 1998;235–237:692–6.
7. Gomez Ribelles JL, Monleon Pradas M, Gallego Ferrer G, Peidro Torres N, Perez Gimenez V, Pissis P, Kyritsis A. Poly(methyl acrylate)/poly(hydroxyethyl acrylate) sequential interpenetrating polymer networks. Miscibility and wáter sorption behavior. J Polym Sci Part B Polym Phys. 1999;37:1587–99.
8. Campillo-Fernandez AJ, Salmeron Sanchez M, Sabater i Serra R, Meseguer Duenas JM, Monleon Pradas M, Gomez Ribelles JL. Water-induced (nano) organization in poly(ethyl acrylate-co-hydroxyethyl acrylate) networks. Eur Polym J. 2008;44: 1996–2004.
9. Kyritsis A, Spanoudaki A, Pandis C, Hartmann L, Pelster R, Shinyashiki N, Rodríguez Hernández JC, Gómez Ribelles JL, Monleón Pradas M, Pissis P. Water and polymer dynamics in poly(hydroxyl ethyl acrylate-*co*-ethyl acrylate) copolymer hydrogels. Eur Polym J. 2011;47:2391–2402.
10. Haraguchi K. Nanocomposite hydrogels. Curr Opin Solid State Mater Sci. 2007;11:47–54.
11. Janovák L, Varga J, Kemény L, Dékány I. Swelling properties of copolymer hydrogels in the presence of montmorillonite and alkylammonium montmorillonite. Appl Clay Sci. 2009;43:260–70.
12. Janovák L, Varga J, Kemény L, Dékány I. The effect of surface modification of layer silicates on the thermoanalytical properties of poly(NIPAAm-co-AAm) based composite hydrogels. J Therm Anal Calorim. 2009;98:485–93.
13. Rodriguez Hernandez JC, Salmeron Sanchez M, Gomez Ribelles JL, Monleon Pradas M. Polymer-silica nanocomposites prepared by sol–gel technique: nanoindentation and tapping mode AFM studies. Eur Polym J. 2007;43:2775–83.
14. Rodriguez Hernandez JC, Monleon Pradas M, Gomez Ribelles JL. Properties of poly(2-hydroxyethyl acrylate)-silica

nanocomposites obtained by the sol–gel process. J Non-Cryst Solids. 2008;354:1900–8.
15. Pandis C, Spanoudaki A, Kyritsis A, Pissis P, Rodriguez Hernandez JC, Gomez Ribelles JL, Monleon Pradas M. Water sorption characteristics of poly(2-hydroxyethyl acrylate)/silica nanocomposite hydrogels. J Polym Sci Part B Polym Phys. 2011;49:657–68.
16. Stathopoulos A, Klonos P, Kyritsis A, Pissis P, Christodoulides C, Rodriguez Hernandez JC, Monleon Pradas M, Gomez Ribelles JL. Water sorption and polymer dynamics in hybrid poly (hydroxyethyl-*co*-ethyl acrylate)/silica hydrogels. Eur Polym J. 2010;46:101–11.
17. Kremer F, Schoenhals A, editors. Broadband dielectric spectroscopy. Berlin: Springer; 2002.
18. Donth E. The glass transition: relaxation dynamics in liquids and disordered materials. Berlin: Springer; 2001.
19. Havriliak S Jr, Havriliak SJ. Dielectric and mechanical relaxation in materials. Munich: Hanser; 1997.
20. Kripotou S, Pissis P, Savelyev YV, Robota LP, Travinskaya TV. Polymer dynamics in polyurethane/clay nanocomposites studied by dielectric and thermal techniques. J Macromol Sci Phys. 2010; 49:86–110.
21. Pelster R, Spanoudaki A, Kruse T. Microstructure and effective properties of nanocomposites: ferrofluids as tunable model systems. J Phys D Appl Phys. 2004;37:307–17.
22. Pissis P, Kyritsis A. Electrical conductivity studies in hydrogels. Solid State Ionics. 1997;97:105–13.
23. Angell CA. Relaxation in liquids, polymers and plastic crystals—strong/fragile patterns and problems. J Non-Cryst Solids. 1991; 131–133:13–31.
24. Fragiadakis D, Pissis P. Glass transition and segmental dynamics in poly(dimethylsiloxane)/silica nanocomposites studied by various techniques. J Non-Cryst Solids. 2007;353:4344–52.
25. Kourkoutsaki Th, Logakis E, Kroutilova I, Matejka L, Nedbal J, Pissis P. Polymer dynamics in rubbery epoxy networks/polyhedral oligomeric silsequioxanes nanocomposites. J Appl Polym Sci. 2009;113:2569–82.
26. Fragiadakis D, Bokobza L, Pissis P. Dynamics near the particle surface in natural rubber–silica nanocomposites. Polymer. 2011;52:3175–3182.
27. Klonos P, Panagopoulou A, Bokobza L, Kyritsis A, Peoglos V, Pissis P. Comparative studies on effects of silica and titania nanoparticles on crystallization and complex segmental dynamics in poly(dimethylsiloxane). Polymer. 2010;51:5490–9.
28. Napolitano S, Wuebbenhorst M. The lifetime of the deviations from bulk behavior in polymers confined at the nanoscale. Nat Commun. 2011;2:260. doi:10.1038/incomms1259.